Photoinduced Charge-Separation and Charge-Recombination Processes of Fullerene[60] Dyads Covalently Connected with Phenothiazine and Its Trimer

Hidehito Kawauchi,[†] Shuichi Suzuki,[†] Masatoshi Kozaki,[†] Keiji Okada,*[,†] D.-M. Shafiqul Islam,[‡] Yasuyuki Araki,*[,‡] Osamu Ito,[‡] and Ken-ichi Yamanaka[§]

Department of Chemistry, Graduate School of Science, Osaka City University, Sugimoto, Sumiyoshi-ku, Osaka 558-8585, Japan, Institute of Multidisciplinary Research for Advanced Materials, Tohoku University, Katahira, Aoba-ku, Sendai, 980-8577 Japan, and Toyota Central R&D Laboratories, Incorporated, Nagakute, Aichi 480-1192, Japan

Received: January 24, 2008; Revised Manuscript Received: April 3, 2008

Photoinduced charge-separation and charge-recombination processes of fullerene[60] dyads covalently connected with phenothiazine and its trimer (PTZ_n-C_{60}, $n = 1$ and 3) with a short amide linkage were investigated. A time-resolved fluorescence study provided evidence of charge separation via the excited singlet state of a C_{60} moiety ($^1C_{60}$*), which displayed high efficiencies in various solvents; Φ^S_{CS} (quantum yield of charge separation via $^1C_{60}$*) = 0.59 (toluene) to 0.87 (DMF) for PTZ_1-C_{60} and 0.78 (toluene) to 0.91 (DMF) for PTZ_3-C_{60}. The transient absorption measurement with a 6 ns time resolution in the visible and near-IR regions showed evidence of the generation of radical ion pairs in relatively polar solvents for both dyads. In nonpolar toluene, only $PTZ_1-{}^3C_{60}$* was observed for PTZ_1-C_{60}, whereas $PTZ_3-{}^3C_{60}$* as well as the radical ion pair state in equilibrium were observed for PTZ_3-C_{60}. The radical ion pairs had relatively long lifetimes: 60 (DMF) to 910 ns (*o*-dichlorobenzene) for $(PTZ)_1^{\bullet+}-C_{60}^{\bullet-}$ and 230 (PhCN) to 380 ns (*o*-dichlorobenzene) for $(PTZ)_3^{\bullet+}-C_{60}^{\bullet-}$. The small reorganization energy (λ) and the electronic coupling element ($|V|$) were estimated by the temperature dependence of the charge-recombination rates, i.e., $\lambda = 0.53$ eV and $|V| = 1.6$ cm^{-1} for $(PTZ)_3^{\bullet+}-C_{60}^{\bullet-}$.

Introduction

Fullerenes such as C_{60} and C_{70} have been well-established as electron acceptors in photoinduced electron-transfer (ET) processes with electron donors.[1–5] Because of the high delocalization of π-electrons in C_{60}, transient absorption bands of the excited singlet states ($^1C_{60}$*), triplet state ($^3C_{60}$*), and the anion radical ($C_{60}^{\bullet-}$) have been reported to appear in the vis and near-IR (NIR) regions.[6–9] Thus, it is extremely important to measure the transient spectra in the vis and NIR regions in order to clarify the mechanism. The application of such techniques has revealed that the relative contribution of the excited singlet states versus the triplet states of fullerenes to the photoinduced ET processes varies with the structure of the substrates in addition to the solvent polarity.[10–12] In the case of mixtures of fullerenes with electron donors, the singlet route generally increases with the concentration of electron donors.[13] In covalently connected fullerene−donor dyads, the excited singlet route for the intramolecular charge-separation (CS) process is usually predominant.[1–5] For specially fixed fullerene−donor systems such as rotaxans, the triplet route for the CS process increases with the distance between C_{60} and the donor.[14,15]

Phenothiazine derivatives are well-known heterocyclic compounds with high electron-donor ability because of their eight (π + n)-electrons in the central ring.[16,17] Molecules and polymers containing a phenothiazine (PTZ) moiety have recently attracted much interest in materials science, because of their potential applicability as electroluminescent and photovoltaic cells.[17–20] Furthermore, intermolecular ET via $^3C_{60}$* has been reported for PTZ derivatives.[21,22] Intramolecular CS processes have also been reported in polar solvent for C_{60}−phenothiazine dyads bridged by flexible linkers;[23] the contribution of CS via the $^3C_{60}$* was studied under magnetic field.

In this study, we have employed C_{60}−phenothiazine dyads in which 10-phenylphenothiazine (PTZ_1) and its trimer, 3,7-bis(10-phenothiazinyl)-10-phenylphenothiazine (PTZ_3),[24] are linked to C_{60} with pyrodinofullerene via a benzamide group that belongs to a short linkage (Chart 1). We report both steady-state and time-resolved fluorescence quenching and transient absorption studies of PTZ_n-C_{60} ($n = 1$ and 3) with a benzamide linkage in various solvents, which provide long-lived radical ion pair (RIP) states. We have also investigated the temperature variation of the ET rates in order to evaluate the Marcus parameters for which a low reorganization energy and a weak electronic coupling element for the charge-recombination (CR) process of $(PTZ)_3^{\bullet+}-C_{60}^{\bullet-}$ are obtained.

Results and Discussion

Materials. PTZ_1-C_{60} and PTZ_3-C_{60} were prepared by applying the Prato reaction[25] to the aldehydes, **4** and **11** (Scheme 1). Compound **1** was synthesized according to the procedure described in the literature,[26] which involves the use of S_8-I_2 for sulfur bridging. For the Pd(0)-mediated cross-coupling reactions of **1**, it is essential to remove the sulfur contaminant involved in the synthesis of **1** through chromatography separation (SiO_2) by using toluene as an eluent. Furthermore, compound **1** should be recrystallized from hot toluene before the Pd(0)-mediated cross-coupling reaction. The synthetic procedures for PTZ_1-C_{60} and PTZ_3-C_{60} are described in the

* Corresponding authors. E-mail: okadak@sci.osaka-cu.ac.jp (K.O.), araki@tagen.tohoku.ac.jp (Y.A.). Tel.: +81-6-6605-2568(K.O.), +81-22-217-5680(Y.A.). Fax: +81-6-6690-2709 (K.O.), +81-22-217-5680 (Y.A.).
† Osaka City University.
‡ Tohoku University.
§ Toyota Central R&D Laboratories.

10.1021/jp800716e CCC: $40.75
Published on Web 06/11/2008

CHART 1

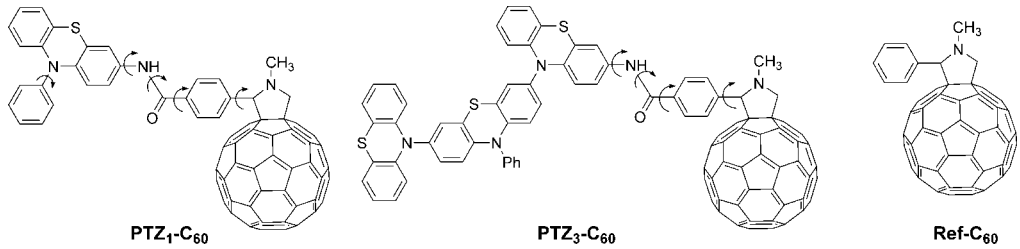

Experimental Section. The synthetic procedures for **2**−**4** and **6**−**11** are described in the Supporting Information.

Optimized Structures and Molecular Orbital Calculations. There are several conformational isomers in PTZ_1−C_{60} and PTZ_3−C_{60}. First, systematic conformation searches for PTZ_1−C_{60} and PTZ_3−C_{60} were carried out by changing the torsion angles (indicated by curved arrows in Chart 1) using Spartan (Wave Function, Inc.) with a molecular mechanics force field (MMFF). The geometry of the most stable conformer obtained by the MMFF method was further refined by the AM1 method (Figure 1). No constraint was applied to PTZ_1−C_{60}, whereas the fixed conformation on the $(PTZ)_3^{\bullet+}$ moiety was applied to PTZ_3−C_{60} (Chart 1) based on the X-ray structure.[24] The final refinement with AM1 for PTZ_3−C_{60} was carried out without geometry fixation. The geometry of these conformers and their highest occupied molecular orbitals (HOMOs) and lowest unoccupied molecular orbitals (LUMOs) are shown in Figure 1, where PTZ_1−C_{60} has an extended form in contrast to the folded form of PTZ_3−C_{60}.

The HOMO of $PTZ_{1,3}$−C_{60} is mainly delocalized on the PTZ ring, whereas the LUMO is delocalized on the C_{60} sphere. The separate distribution of the HOMO and LUMO to the donor and acceptor, respectively, suggests the CS state, $(PTZ)_{1,3}^{\bullet+}$−$C_{60}^{\bullet-}$, in the first singlet excited state. The consideration is in good agreement with the time-dependent density functional theory (TD-DFT) calculations (B3LYP/6-31G(d)) for the first singlet excited state (Supporting Information). No overlap between HOMO and LUMO is compatible with the fact that there is no appreciable charge-transfer (CT) band in these dyads (vide infra). The center-to-center distance (R_{CC}) between the radical cation and the radical anion was approximated as the distance between the center of C_{60} and the center of the central ring of the PTZ, which was estimated to be 13.0 Å for $(PTZ)_1^{\bullet+}$−$C_{60}^{\bullet-}$ and 10.5 Å for $(PTZ)_3^{\bullet+}$−$C_{60}^{\bullet-}$. The larger R_{CC} for $(PTZ)_1^{\bullet+}$−$C_{60}^{\bullet-}$ reflects the extended structure (Figure 1).

SCHEME 1

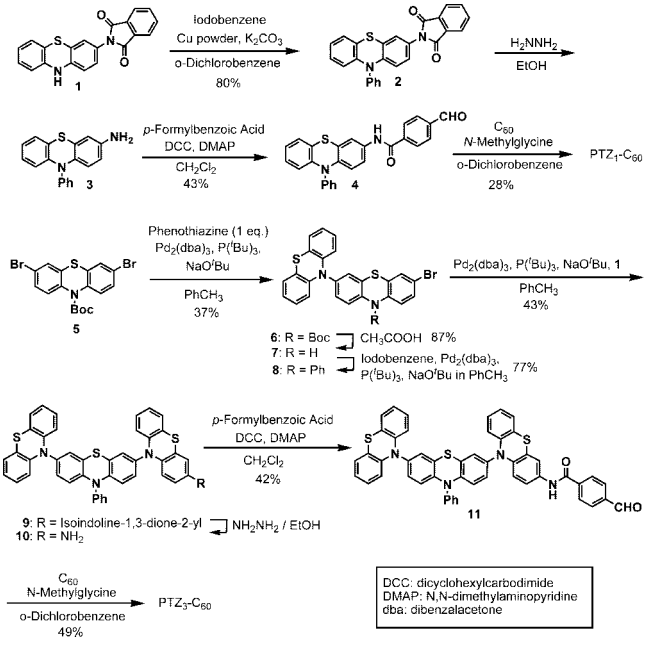

Redox Potentials and Free-Energy Changes. The cyclic voltammograms showed reversible peaks; the first oxidation potential ($E_{ox}^{1/2}$) and the first reduction potential ($E_{red}^{1/2}$) were determined to be 0.18 and −1.03 V for PTZ_1−C_{60}, and 0.09 and −1.03 V versus ferrocene/ferrocene$^{\bullet+}$ (Fc/Fc$^{\bullet+}$) for PTZ_3−C_{60} in PhCN (Supporting Information Figure S1). The energies of the RIPs (ΔG_{RIP}) in PhCN (dielectric constant, ε = 25.7) were calculated using the Rehm−Weller approximation as follows:[27a]

$$\Delta G_{RIP} = E_{ox}^{1/2}(PTZ_n) - E_{red}^{1/2}(C_{60}) - 14.4/(\varepsilon R_{CC}) \quad (1)$$

The ΔG_{RIP} values in DMF (ε = 36.7) and *o*-DCB (9.93) were estimated by adding a correction term $(14.4/r)(1/\varepsilon - 1/\varepsilon_{ref})$ to eq 1,[27b] where ε_{ref} refers to the dielectric constant of PhCN. An averaged value of 5 Å[27b] for the ionic effective radius r was used in the calculation. The ΔG_{RIP} values in toluene (ε = 2.38) were estimated using the redox potentials in CH_2Cl_2 (ε = 8.93; $E_{ox}^{1/2}$ = 0.15 V and $E_{red}^{1/2}$ = −1.13 V for PTZ_1−C_{60}, and $E_{ox}^{1/2}$ = 0.06 V and $E_{red}^{1/2}$ = −1.13 V for PTZ_3−C_{60}) rather than using those in PhCN in order to obtain a better comparison of redox potentials in solvents whose polarities are not very different.

The free-energy changes for the CS process via $^1C_{60}$* (ΔG^S_{CS}) and via $^3C_{60}$* (ΔG^T_{CS}) were calculated from eq 2 using the energy levels of the excited singlet state of C_{60} (E^S_{0-0} = 1.72 eV) and the triplet state of C_{60} (E^T_{0-0} = 1.50 eV):[1-5]

$$\Delta G_{CS} = \Delta G_{RIP} - E_{0-0} \quad (2)$$

The ΔG^S_{CS} values listed in Table 1 are all negative. The ΔG^T_{CS} values in polar solvents are also negative, predicting

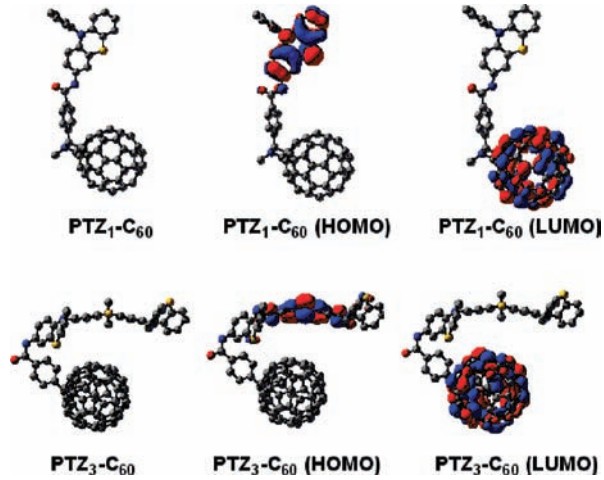

Figure 1. Structures of the most stable conformers of PTZ_1−C_{60} and PTZ_3−C_{60} and their HOMOs and LUMOs.

exothermic CS processes via the $^3C_{60}$* moiety. The ΔG^T_{CS} value in nonpolar toluene was positive for PTZ_1-C_{60}, whereas it was almost zero for PTZ_3-C_{60}. The ΔG_{CS} values for PTZ_3-C_{60} are more negative than those for PTZ_1-C_{60} in the same solvents, reflecting smaller $E_{ox}^{1/2}$ and R_{CC} values of PTZ_3-C_{60}. Energy diagrams can be constructed on the basis of these thermodynamic data (Supporting Information Figure S2).

Steady-State Absorption Spectra. The absorptions of PTZ_3-C_{60} in the vis region are mainly due to the C_{60} moiety, whereas the absorptions in the UV region consist of overlapped bands due to both the C_{60} and the PTZ_3 moieties (Figure 2). The PTZ_3 moiety has no strong absorption band in a longer wavelength region than 400 nm. A weak band around 700 nm and a sharp absorption band at 431 nm are characteristic bands of the fulleropyrolidine.[1–5] A similar absorption spectrum was observed for PTZ_1-C_{60} (Supporting Information Figure S3). In both dyads, no appreciable CT band appeared, which suggests that the electronic interaction between the C_{60} and PTZ moieties is very small in the ground state. Therefore, the 532 nm laser light used for the laser flash photolysis selectively excites the C_{60} moiety. The laser lights at 431 and 400 nm for fluorescence lifetime measurements also selectively excite the C_{60} moiety.

In order to assign transient absorptions, we have measured the absorptions of the radical cations under electrochemical conditions in CH_2Cl_2. The absorption bands of $(PTZ)_1^{\bullet+}$ and $(PTZ)_3^{\bullet+}$ were observed at 606 and 944 nm, respectively, with an applied potential of 0.3−0.5 V versus Fc/Fc^+ (Supporting Information Figure S4). The distinct difference in absorptions between $(PTZ)_1^{\bullet+}$ and $(PTZ)_3^{\bullet+}$ has already been clarified.[24] The absorption of ref-C_{60} radical anion around 1000 nm has already been established.[1–5]

TABLE 1: Energies of Radical Ion Pairs (ΔG_{RIP}) and Free-Energy Changes for Charge Separation via $^1C_{60}$* (ΔG^S_{CS}) and via $^3C_{60}$* (ΔG^T_{CS})

compd	solvent	ΔG_{RIP}/eV[a]	$-\Delta G^S_{CS}$/eV	$-\Delta G^T_{CS}$/eV
PTZ_1-C_{60}	toluene	1.70[b]	0.02	−0.20
	o-DCB	1.28	0.44	0.22
	PhCN	1.17	0.55	0.33
	DMF	1.15	0.57	0.35
PTZ_3-C_{60}	toluene	1.50[b]	0.22	0.00
	o-DCB	1.16	0.56	0.34
	PhCN	1.07	0.65	0.43
	DMF	1.05	0.67	0.45

[a] The ΔG_{RIP} values were estimated according to the methods described in text. [b] The ΔG_{RIP} values in toluene may contain considerable errors.

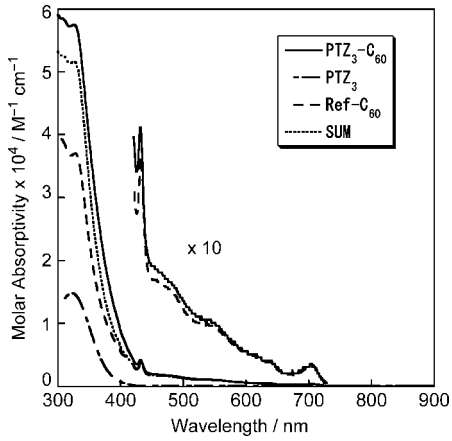

Figure 2. Absorption spectra of PTZ_3-C_{60} and its components in PhCN.

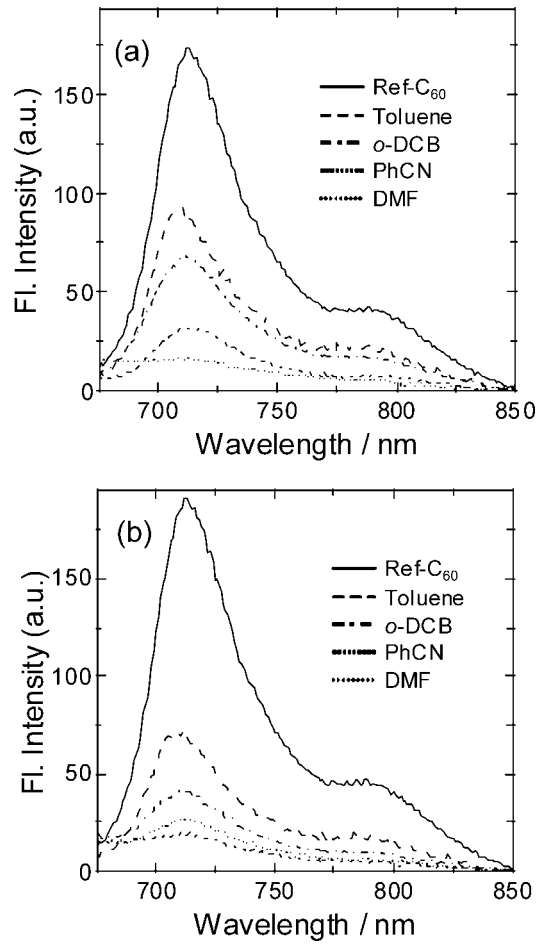

Figure 3. Steady-state fluorescence spectra of (a) PTZ_1-C_{60} and (b) PTZ_3-C_{60} in various solvents at room temperature in comparison with ref-C_{60} ; λ_{ex} = 431 nm.

Steady-State Fluorescence Spectra. Parts a and b of Figure 3 show the steady-state fluorescence spectra of PTZ_1-C_{60} and PTZ_3-C_{60}, respectively, together with that of ref-C_{60}. The fluorescence spectra ($\lambda_{EM,max}$ = 715 nm) are very similar in shape to that of ref-C_{60}. The intensities of the fluorescence of PTZ_n-C_{60} were found to be considerably smaller than that of ref-C_{60} under identical excitation light intensity and absorbance at the excitation wavelength of 431 nm. The quenching of the fluorescence of $PTZ_n-{}^1C_{60}$* indicates the occurrence of the intramolecular CS process. The efficiency of fluorescence quenching increases with an increase in the polarity of the solvent. Considerable fluorescence quenching was also observed in toluene, suggesting the CS process in this nonpolar solvent. PTZ_3-C_{60} had higher quenching efficiencies than PTZ_1-C_{60} in all solvents, which supports the higher electron-donating ability of the PTZ_3 moiety as compared to the PTZ_1 moiety.

Fluorescence Lifetime Measurements. The time-resolved fluorescence spectra measured with the streak-scope method showed a similar trend to the steady-state emission spectra. The fluorescence time profiles provide direct information about the fluorescence quenching rates. Parts a and b of Figure 4 show the decaying time profiles of the fluorescence intensity of PTZ_1-C_{60} and PTZ_3-C_{60}, respectively. The fluorescence decay of ref-C_{60} was monoexponential; the lifetime of ref-$^1C_{60}$* was determined to be 1400 ps from the decay curve. The fluorescence decays of PTZ_1-C_{60} and PTZ_3-C_{60} were curve-fitted by an almost monoexponential function, giving short lifetimes (>90%, τ_F in Table 2). The decays included a minor long

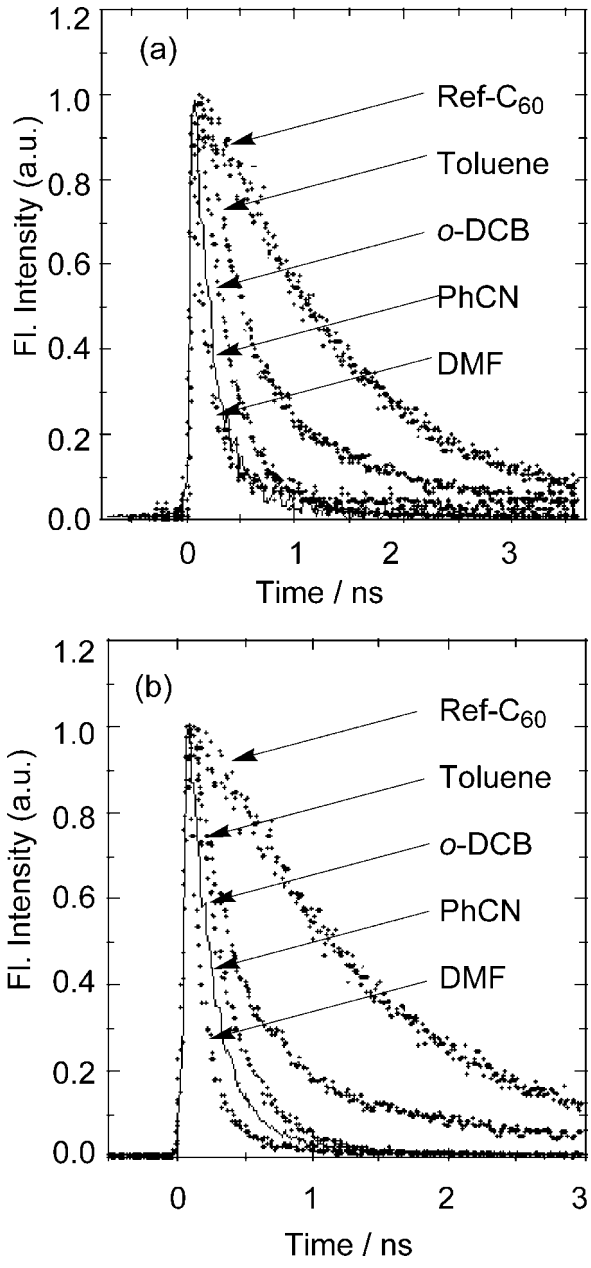

Figure 4. Fluorescence decay time profiles in 700−750 nm region for (a) PTZ_1−C_{60} and (b) PTZ_3−C_{60} in various solvents with a reference of ref-C_{60}; λ_{ex} = 400 nm, and intensities were normalized at initial maxima.

TABLE 2: Fluorescence Lifetime (τ_F) of $^1C_{60}$* Moiety, Charge-Separation Rate Constant (k^S_{CS}), and Charge-Separation Quantum Yield (Φ^S_{CS}) via $^1C_{60}$* Moiety at Room Temperature

compd	solvent	τ_F/ps	k^S_{CS}/s^{-1} [a]	Φ^S_{CS} [a]
PTZ_1−C_{60}	toluene	575	1.0×10^9	0.59
	o-DCB	305	2.6×10^9	0.78
	PhCN	192	4.5×10^9	0.86
	DMF	155	6.2×10^9	0.87
PTZ_3−C_{60}	toluene	305	2.6×10^9	0.78
	o-DCB	280	2.9×10^9	0.80
	PhCN	165	5.4×10^9	0.88
	DMF	130	7.0×10^9	0.91

[a] $k^S_{CS} = (1/\tau_F)_{sample} - (1/\tau_F)_{ref}$, $\Phi^S_{CS} = [(1/\tau_F)_{sample} - (1/\tau_F)_{ref}]/(1/\tau_F)_{sample}$. $(\tau_F)_{ref}$ = 1.4 ns.

component (<10%, ca. 1400 ps), which may be attributed to some conformers[28] or decomposition products during photolysis, although thin-layer chromatography (TLC) analysis did not show clear decomposition products after the fluorescence time profile measurements. The short component represents the rate constant of the CS process from PTZ_n−$^1C_{60}$*.[29] The rate constant (k^S_{CS}) and the quantum yield (Φ^S_{CS}) of the CS process were estimated from the reduction in the lifetime of the fluorescence, as summarized in Table 2. As the polarity of the solvent increased, the values of k^S_{CS} and Φ^S_{CS} increased. The lowest values were obtained in toluene, where k^S_{CS} = 1.0 (2.6) × 10^9 s^{-1} and Φ^S_{CS} = 0.59 (0.78) for PTZ_1−C_{60} (number in parenthesis is for PTZ_3−C_{60}). PTZ_3−C_{60} had slightly larger k^S_{CS} values [(2.6−7.0) × 10^9 s^{-1}] and Φ^S_{CS} values (0.78−0.91) than PTZ_1−C_{60} [k^S_{CS} = (1.0−6.2) × 10^9 s^{-1} and Φ^S_{CS} = 0.59−0.87], which was in agreement with the steady-state fluorescence measurements.

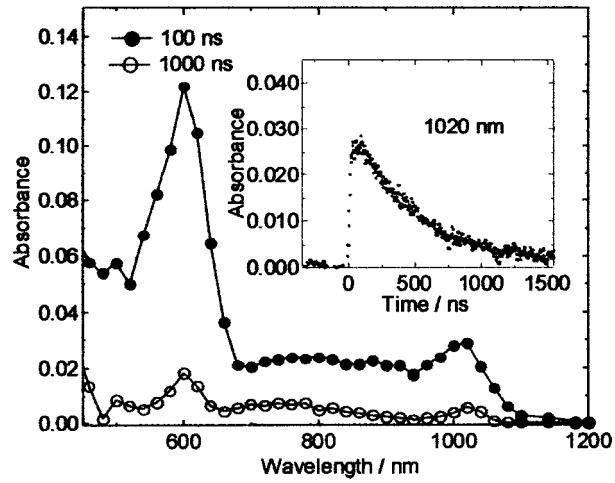

Figure 5. Transient absorption spectra of PTZ_1−C_{60} (0.15 mM) in Ar-saturated PhCN with 532 nm excitation at room temperature. Inset: a decay curve at 1020 nm.

TABLE 3: Charge-Recombination Rate Constant (k_{CR}) and Lifetime (τ_{RIP}) of $(PTZ)_n^{\bullet+}$−$C_{60}^{\bullet-}$ at Room Temperature

compd	solvent	k_{CR}/s^{-1}	τ_{RIP}/ns	k_{CS}/k_{CR}
$(PTZ)_1^{\bullet+}$−$C_{60}^{\bullet-}$	toluene			
	o-DCB	1.1×10^6	910	2360
	PhCN	2.9×10^6	350	2250
	DMF	1.7×10^7	60	360
$(PTZ)_3^{\bullet+}$−$C_{60}^{\bullet-}$	toluene	(2.3×10^6)[a]	(430)[a]	
	o-DCB	2.6×10^6	380	1120
	PhCN	4.4×10^6	230	1540
	DMF	3.8×10^6	260	1840

[a] Assuming an equilibrium between $(PTZ)_3^{\bullet+}$−$C_{60}^{\bullet-}$ and PTZ_3−$^3C_{60}$*, k^T_{CS} = 6.0 × 10^5 s^{-1}, and k_{CR} and τ_{RIP} were evaluated (see Supporting Information Figure S7).

Transient Absorption Studies of PTZ_n−C_{60}. Figure 5 shows the transient absorption spectra of PTZ_1−C_{60} in PhCN by laser excitation with 532 nm. The absorption bands of $(PTZ)_1^{\bullet+}$ at 600 nm[24] and $C_{60}^{\bullet-}$ at 1020 nm[1–5] were clearly observed, suggesting the formation of $(PTZ)_1^{\bullet+}$−$C_{60}^{\bullet-}$. No absorption due to the $^3C_{60}$* moiety was observed. The RIP was rapidly generated within the 6 ns laser light pulse (inset of Figure 5). From the decay at 1020 nm, the k_{CR} value was evaluated to be 2.9 × 10^6 s^{-1}, which corresponds to a lifetime (τ_{RIP}) of 350 ns for $(PTZ)_1^{\bullet+}$−$C_{60}^{\bullet-}$ in PhCN. The same values were obtained for the decay at 600 nm (Supporting Information Figure S5). For other polar solvents, similar transient spectra and time profiles were observed, giving the k_{CR} and τ_{RIP} values listed in Table 3, although a shorter lifetime was observed in DMF for PTZ_1−C_{60}.

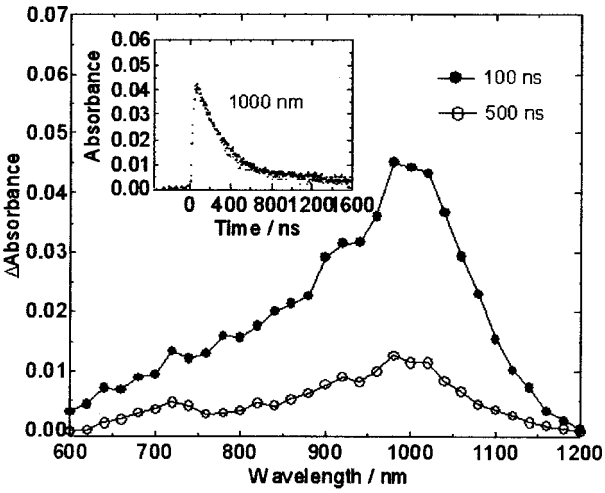

Figure 6. Nanosecond transient absorption spectra of PTZ_3-C_{60} (0.15 mM) in Ar-saturated PhCN with 532 nm excitation at room temperature. Inset: decay curve at 1000 nm.

A broad transient absorption band was observed in the 750−1200 nm region for PTZ_3-C_{60} in PhCN (Figure 6) with a maximum around 1000 nm due to an overlap of the absorption of $(PTZ)_3^{\bullet+}$ (λ_{max} = 944 nm in Supporting Information Figure S4, ε = 28 300 M^{-1} cm^{-1} in CH_2Cl_2)[24] and ref-$C_{60}^{\bullet-}$ (λ_{max} = 1000 nm, ε_{max} = 4700 M^{-1} cm^{-1} in PhCN).[30] The observed absorption band of $(PTZ)_3^{\bullet+}$ at 1000 nm has been attributed to the delocalization of a hole on the central PTZ ring,[24] suggesting that the formation of an RIP as well as the hole delocalization takes place within the 6 ns laser light pulse in PhCN. From the decay at 1000 nm, the k_{CR} value was estimated to be 4.4×10^6 s^{-1} (τ_{RIP} = 230 ns) for $(PTZ)_3^{\bullet+}-C_{60}^{\bullet-}$ in PhCN. In other polar solvents, similar transient spectra were observed, giving the corresponding k_{CR} and τ_{RIP} values as summarized in Table 3. The variation in the τ_{RIP} values for $(PTZ)_3^{\bullet+}-C_{60}^{\bullet-}$ is in a rather narrow range (230−380 ns) in the polar solvents, DMF−*o*-DCB, whereas the larger variation of the τ_{RIP} values (60−910 ns) was observed for $(PTZ)_1^{\bullet+}-C_{60}^{\bullet-}$ in the same set of solvents, suggesting different mechanisms of electron transfer for these dyads. Considering the conformations of these dyads (Figure 1), the electron transfer is likely to occur via a through-bond manner for PTZ_1-C_{60} and via a through-space manner for PTZ_3-C_{60}. The smaller τ_{RIP} values of $(PTZ)_3^{\bullet+}-C_{60}^{\bullet-}$ in comparison with those of $(PTZ)_1^{\bullet+}-C_{60}^{\bullet-}$ in *o*-DCB and PhCN are also compatible with this consideration and with the shorter R_{CC} (10.5 Å) for $PTZ_3^{\bullet+}-C_{60}^{\bullet-}$ (R_{CC} = 13.0 Å for $(PTZ)_1^{\bullet+}-C_{60}^{\bullet-}$).

For PTZ_1-C_{60} in toluene, an intense absorption band was observed at ca. 700 nm (Supporting Information Figure S6), which is attributed to $^3C_{60}$* decaying exclusively to the ground state with a lifetime of 1500 ns. No apparent absorption due to $(PTZ)_1^{\bullet+}-C_{60}^{\bullet-}$ was observed around 600 nm, which suggests that $^1[(PTZ)_1^{\bullet+}-C_{60}^{\bullet-}]$ is short-lived (less than the 6 ns laser light pulse) due to the rapid CR process, undergoing to $PTZ_1-{}^3C_{60}$* via an intersystem crossing[31] and/or to the ground state in toluene.

Transient absorption spectra for the excitation of PTZ_3-C_{60} in toluene showed a 700 nm band due to the $^3C_{60}$* moiety as well as a weak band that appeared near 1000 nm due to $(PTZ)_3^{\bullet+}$ and $C_{60}^{\bullet-}$ in the RIP (Figure 7). Despite of the initial decay of the 700 nm band due to $^3C_{60}$*, the absorption at 1000 nm continues to rise and reaches to the maximum intensity ca. 500 ns after the laser pulse, indicating that $(PTZ)_3^{\bullet+}-C_{60}^{\bullet-}$ is formed via $PTZ_3-{}^3C_{60}$* in nonpolar toluene. The rise and decay of the transient absorption bands at 1000 nm and the two-step decay

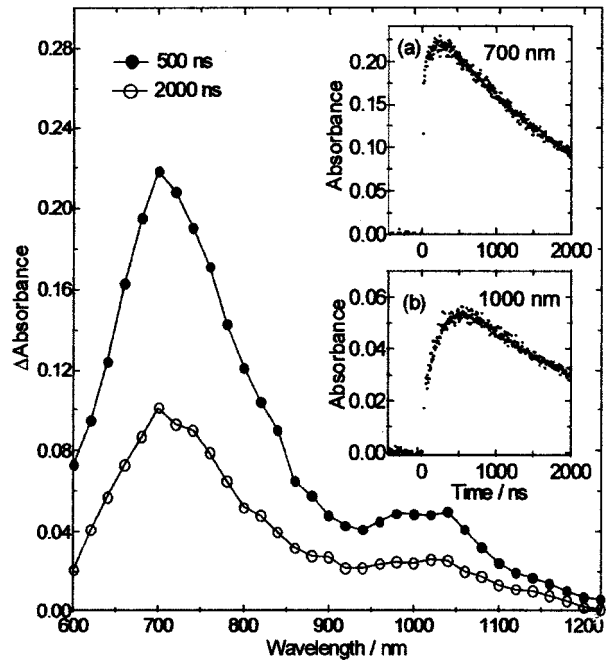

Figure 7. Time-resolved nanosecond transient absorption spectra of PTZ_3-C_{60} (0.15 mM) in Ar-saturated toluene obtained by 532 nm laser light irradiation. Inset: absorption time profiles at (a) 700 and (b) 1000 nm.

of the 700 nm band are consistent with a mechanism including an equilibrium between $(PTZ)_3^{\bullet+}-C_{60}^{\bullet-}$ and $PTZ_3-{}^3C_{60}$* with similar energy levels.[32] The analysis of the decay processes with the equilibrium is shown in Supporting Information Figure S7. The CS rate via the $^3C_{60}$* moiety (k^T_{CS}) was estimated to be 6.0×10^5 s^{-1}, and the CR rate (k_{CR}) giving $PTZ_2-{}^3C_{60}$* had a value of 2.3×10^6 s^{-1}, which corresponds to τ_{RIP} = 430 ns. The relation of $k^T_{CS} < k_{CR}$ qualitatively accords with the observation that the maximal concentration of the $(PTZ)_3^{\bullet+}-C_{60}^{\bullet-}$ is lower than that of $PTZ_3-{}^3C_{60}$*[33] by a factor of about 1/10 if the values of ε_{1000nm} [33 000 M^{-1} cm^{-1} as a summation of $(PTZ)_3^{\bullet+}$ (28 300 M^{-1} cm^{-1}),[24] $C_{60}^{\bullet-}$ (4700 M^{-1} cm^{-1})[30]] and ε_{700nm} of $^3C_{60}$* (16 100 M^{-1} cm^{-1})[34] are taken into account.

Temperature Effect of PTZ_3-C_{60}. The present study provides a good example of the CR system. The decay rates of $(PTZ)_n^{\bullet+}-C_{60}^{\bullet-}$ slowed down with lowering the temperature, suggesting an appreciable activation energy ($\Delta G^{\ddagger}_{CR}$) for the CR process. Fortunately, the dyad PTZ_3-C_{60} had a moderate solubility in THF even at a low temperature of ca. −50 °C. We have studied the temperature dependence of the rate constants on the CR process. The polarity of THF (ε = 7.52) is roughly similar to that of *o*-DCB (ε = 9.93). According to the semiclassical Marcus equation,[35] the ET rate constant (k_{ET}) can be described as follows:

$$\ln(k_{ET}T^{1/2}) = \ln\{2\pi^{3/2}|V|^2/[h(\lambda k_B)^{1/2}]\} - \Delta G^{\ddagger}/(k_BT) \quad (3)$$

where T, h, and k_B denote the absolute temperature, Planck constant, and Boltzmann constant, respectively; $|V|$, λ, and $\Delta G^{\ddagger}$ refer to the electron coupling matrix element, reorganization energy, and Gibbs activation energy in the Marcus theory, respectively. The plots of $\ln(k_{CR}T^{1/2})$ against $1/T$ for $(PTZ)_3^{\bullet+}-C_{60}^{\bullet-}$ show a straight line (Figure 8). From the slope of the plots in Figure 8, $\Delta G^{\ddagger}_{CR}$ was evaluated to be 0.138 eV. The λ value was calculated to be 0.53 eV from eq 4,[35] using $\Delta G_{CR} = -\Delta G_{RIP} = -1.07$ eV in THF:

$$\Delta G^{\ddagger}_{CR} = \frac{(\Delta G_{CR} + \lambda)^2}{4\lambda} \quad (4)$$

Such a small λ value is characteristic of the ET process of spherical fullerene molecules.[36] Furthermore, the coupling constant ($|V|$) was evaluated to be 1.6 cm^{-1} from the intercept of Figure 8. This small value of $|V|$ is probably due to the through-space interaction between the central $PTZ^{\bullet+}$ and $C_{60}^{\bullet-}$ moiety (Figure 1). The small $|V|$ value supports the slow CR rate and the long τ_{RIP} of $(PTZ)_3^{\bullet+}-C_{60}^{\bullet-}$ in combination with the small λ value.

Spin-Multiplicity of RIPs. The relatively long lifetimes (τ_{RIP}) in the polar solvents (*o*-DCB and PhCN, Table 3) for both dyads suggest a triplet character of the RIP states; in the related system, PTZ−C_{60} bridged by a flexible methylene chain $(CH_2)_{10}$ through an oxyphenylpyrodino group exhibits the lifetime of 120 ns in benzonitrile, which becomes longer by about twice under an external magnetic field, showing that the RIP is in the triplet state.[23] The reported lifetimes in the methylene-linked PTZ−C_{60} are in a range of the lifetimes in the present study (60−910 ns, Table 3), suggesting that the observed RIPs in the present study are also in triplet states.

In principle, it is considered that an RIP with a singlet spin character can be generated via $PTZ_n-{}^1C_{60}$* with a fraction of Φ^S_{CS}. However, $^1[(PTZ)_n^{\bullet+}-C_{60}^{\bullet-}]$ may undergo a rapid spin conversion to yield $^3[(PTZ)_n^{\bullet+}-C_{60}^{\bullet-}]$. Such an intersystem crossing within RIPs has generally been observed in systems that have a small electronic matrix element $|V|$.[37,38] In the present case, the $|V|$ value is a few cm^{-1} for PTZ_3-C_{60}, which allows partial spin conversion within the RIP state.[37] Thus, long-lived RIPs acquire a triplet spin character via an intersystem crossing within the RIP state, i.e., $^1[(PTZ)_n^{\bullet+}-C_{60}^{\bullet-}] \rightarrow {}^3[(PTZ)_n^{\bullet+}-C_{60}^{\bullet-}]$ in the polar solvents. The pathway of $^1[(PTZ)_n^{\bullet+}-C_{60}^{\bullet-}] \rightarrow PTZ_n-{}^3C_{60}$* in the polar solvents is endothermic.

In toluene, $PTZ_3-{}^3C_{60}$* may be formed from $PTZ_3-{}^1C_{60}$* via an intersystem crossing within the C_{60} moiety and/or from $^1[(PTZ)_3^{\bullet+}-C_{60}^{\bullet-}]$ ($\Phi^S_{CS} = 0.78$) via a CR process accompanied by an intersystem crossing.[31] In the latter case, the absorption of the RIP is very minor in the initial stage as judged from the low absorbance around 1000 nm within 10 ns after the laser pulse (Figure 7); this suggests a rapid transformation of $^1[(PTZ)_3^{\bullet+}-C_{60}^{\bullet-}] \rightarrow PTZ_3-{}^3C_{60}$*, which would have a relatively long lifetime to equilibrate with $^3[(PTZ)_3^{\bullet+}-C_{60}^{\bullet-}]$. The small population of $^3[(PTZ)_3^{\bullet+}-C_{60}^{\bullet-}]$ suggests that the CS process from $PTZ_3-{}^3C_{60}$* is probably slightly endothermic.

Conclusion

For two dyads, PTZ_n-C_{60} (n = 1 or 3), the photoinduced CS and CR processes were confirmed by using time-resolved spectroscopic methods. The time-resolved fluorescence study provided information about the CS processes via $^1C_{60}$* for both dyads in various solvents. The RIP states were observed for both dyads in the polar solvents in the transient absorption measurement. In nonpolar toluene, only $PTZ_1-{}^3C_{60}$* was observed for PTZ_1-C_{60}; $PTZ_3-{}^3C_{60}$* and the RIP state in equilibrium were observed for PTZ_3-C_{60}.

The RIP states had lifetimes of ca. 100−1000 ns for $(PTZ)_1^{\bullet+}-C_{60}^{\bullet-}$ and 300−400 ns for $(PTZ)_3^{\bullet+}-C_{60}^{\bullet-}$ with a narrower time range which remained almost invariant. The latter value suggests the CR process via a through-space manner that is consistent with the folded conformation of PTZ_3-C_{60}. These long lifetimes suggest that the RIP states would have triplet a character induced by intersystem crossing within the RIP states in the polar solvents or by the equilibrium with $PTZ_3-{}^3C_{60}$* in toluene. The reorganization energy (λ) and the electronic coupling element (V) were determined as 0.53 eV and 1.6 cm^{-1}, respectively, from the temperature dependence of the CR rates of $(PTZ)_3^{\bullet+}-C_{60}^{\bullet-}$. The small value of $|V|$ is consistent with the mechanism of intersystem crossing within the RIP states.

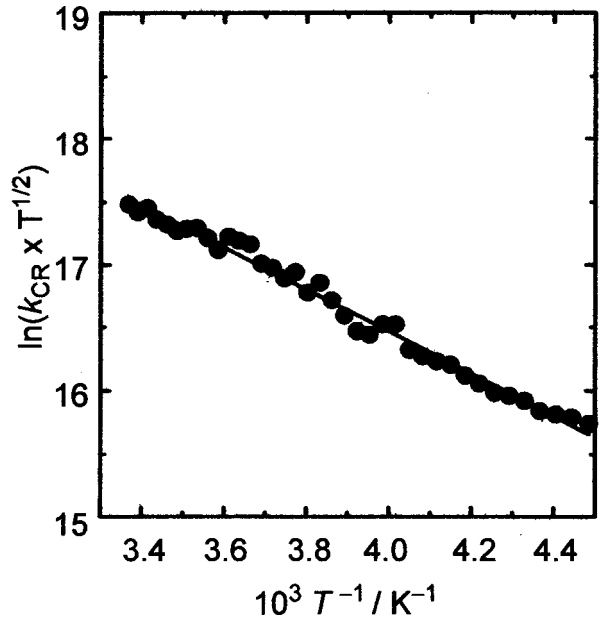

Figure 8. Semiclassical Marcus (modified Arrhenius) plots of the temperature dependence of the k_{CR} values for $(PTZ)_3^{\bullet+}-C_{60}^{\bullet-}$ in THF.

The ratios of k_{CS}/k_{CR} are considered to be a measure of effectiveness in the photoinduced CS processes; these values were found to lie in the range of 1000−2000 (Table 3). Thus, the generated electron−hole pair can be applied to further chemical, electrochemical, and catalytic reactions as light-harvesting systems.

Experimental Section

Materials. Synthetic procedures for PTZ_1-C_{60} and PTZ_3-C_{60} are described below (see the Supporting Information for other compounds).

Synthesis of PTZ_1-C_{60}. To a 100 mL two-necked flask were added compound **4** (76 mg, 0.18 mmol), C_{60} (130 mg, 0.18 mmol), *N*-methylglycine (48 mg, 0.54 mmol), and dry *o*-dichlorobenzene (40 mL). The mixture was refluxed for 2 h with stirring. *o*-Dichlorobenzene (10 mL) was added to the hot reaction mixture. After cooling to room temperature, the mixture was filtered. The filtrate was concentrated, and the residue was purified by chromatographic separation (SiO_2 with toluene using toluene as a first eluent to remove C_{60} and CH_2Cl_2 as a second eluent to elute the product). The obtained black powder was dissolved by a minimum amount of carbon disulfide and precipitated by adding ether. Thus obtained black powder after drying gave satisfactory analytical data as PTZ_1-C_{60} (58 mg, 28%). PTZ_1-C_{60}: $C_{88}H_{23}N_3OS$, MW 1170.21, black powder, mp >300 °C. ^1H NMR (400 MHz, $CDCl_3$) δ 7.97−7.87 (m, 4H), 7.60 (t, J = 7.6 Hz, 3H), 7.47 (t, J = 7.6 Hz, 1H), 7.39−7.34 (m, 3H), 7.06 (d, J = 9.6 Hz, 1H), 7.00 (dd, J = 7.6 Hz, 1.6 Hz 1H), 6.87−6.77 (m, 2H), 6.18−6.15 (m, 2H), 5.02−4.99 (m, 2H), 4.29 (d, J = 9.6 Hz, 1H), 2.81 (s, 3H). IR (KBr, cm^{-1}) 2779 (w), 1655 (m), 1576 (w), 1491 (s), 1466 (s), 1439 (m), 1394 (w), 1300 (m), 1248 (m), 1221 (w), 744 (m), 705 (w), 526 (s). HRMS (FAB) *m/z* calcd for $C_{88}H_{23}N_3OS$: 1169.1562. Found: 1169.1559.

Synthesis of PTZ_3-C_{60}. To a 50 mL two-necked flask were added compound **11** (65 mg, 0.080 mmol), C_{60} (61 mg, 0.080 mmol), *N*-methylglycine (30 mg, 0.32 mmol), and dry *o*-dichlorobenzene (16 mL). The mixture was refluxed for 2 h with stirring. *o*-Dichlorobenzene (10 mL) was added to the hot reaction mixture. The mixture was filtered, and the filtrate was concentrated under reduced pressure. The residue was purified by chromatographic separation (SiO_2 with toluene using toluene as a first eluent to remove C_{60} and CH_2Cl_2 as a second eluent to elute the product). The obtained black powder was dissolved by a minimum amount of chloroform. Diethyl ether was added to the chloroform solution to give precipitates (56 mg, 45%). PTZ_3-C_{60}; $C_{112}H_{37}N_5OS_3$, MW 1564.72, black powder, mp >300 °C. ^{1}H NMR (400 MHz, $CDCl_3$) δ 7.97−7.86 (m, 4H), 7.72−7.68 (m, 2H), 7.64 (s, 1H), 7.59−7.51 (m, 3H), 7.31 (s, 1H), 7.09 (d, $J = 8.8$ Hz, 1H), 7.04−7.02 (m, 2H), 6.99−6.95 (m, 3H), 6.90−6.77 (m, 8H), 6.37−6.30 (m, 6H) 5.02−5.00 (m, 2H), 4.29 (d, $J = 9.6$ Hz, 1H), 2.81 (s, 3H). IR (KBr, cm^{-1}) 2787 (w), 1684 (w), 1576 (w), 1491 (m), 1464 (s), 1441 (m), 1394 (w), 1300 (m), 1232 (m), 744 (m), 526 (m). HRMS (FAB) *m/z* calcd for $C_{112}H_{37}N_5OS_3$: 1563.2160. Found: 1563.2175.

Apparatus. Molecular orbital calculations were performed with Spartan (Wave function, Inc.). Redox potentials of PTZ_1-C_{60} were measured by a voltammetric analyzer (ALS 610A) in a conventional three-electrode cell equipped with a glassy carbon as a working electrode and a platinum wire as a counter electrode, and SCE reference electrode. The measurement was carried out with a sweep rate of 100 mV/s in suitable solvents in the presence 0.1 M of tetrabutylammonium perchlorate (Nakalai Tesque) as electrolyte under inert conditions. All the potentials were corrected by the Fc/Fc^+ potential.

Steady-state absorption and fluorescence spectra were measured with a JASCO/V-570 spectrophotometer and a Shimadzu RF-5300 PC spectrofluorophotometer.

Transient absorption spectra in the vis and NIR regions were obtained by using the laser flash photolysis apparatus. The sample solutions were deaerated by bubbling with argon before measurements and illuminated with the SHG (532 nm) light of a Nd:YAG laser (Quanta-Ray; 6 ns fwhm). A module using Ge-APD (600−1600 nm) was employed as a detector for monitoring the light from a pulsed Xe lamp.[5] The laser photolysis was performed in a rectangular quartz cell with a 10 mm optical path in temperature variation equipments. Room temperature was at 23 ± 1 °C. Details of the experimental procedures are described elsewhere.[5]

Acknowledgment. K.O. thanks the Iketani Science and Technology Foundation (No. 0191002-A) for financial support.

Supporting Information Available: Synthetic procedures and compound data for **2**−**4** and **6**−**11**, figures of cyclic voltammograms of PTZ_n-C_{60} (Figure S1), energy diagram of PTZ_n-C_{60} (Figure S2), UV−vis absorption spectra of PTZ_n-C_{60} (Figure S3), spectral change during electrochemical oxidation of PTZ_n-C_{60} (Figure S4), a decay curve at 600 nm for the excitation of PTZ_1-C_{60} in PhCN (Figure S5), transient absorption spectra of PTZ_1-C_{60} in toluene (Figure S6), the equilibrium scheme, decay curves, and analytical equations for the photolysis of PTZ_3-C_{60} (Figure S7), and the results of TD-DFT B3LYP/6-31G* calculations for PTZ_1-C_{60} and PTZ_3-C_{60}. This material is available free of charge via the Internet at http://pubs.acs.org.

References and Notes

(1) Foote, C. S. *Physics and Chemistry of the Fullerenes*; Prassides, K., Ed.; NATO ASI Series; Kluwer Academic Publishers: Dordrecht, The Netherlands, 1994; Vol. C-443, pp 79−96.

(2) Ito, O. *Res. Chem. Intermed.* **1997**, *23*, 389.

(3) Maggini, M.; Guldi, D. M. In *Molecular and Supramolecular Photochemistry*; Ramamurthy, V.; Schanze, K. S., Eds.; Marcel Dekker: New York, 2000; Vol. 4, pp 149−196.

(4) Guldi, D. M.; Kamat, P. V. In *Fullerenes, Chemistry, Physics and Technology*; Kadish, K. M.; Ruoff, R. S. Eds.; Wiley-Interscience: New York, 2000; pp 225−281.

(5) Araki, Y.; Ito, O. In *Handbook of Organic Electronics and Photonics*; Nalwa, H. S., Ed.; American Scientific Publishers: Stevenson Ranch, CA, 2008; Vol. 2, Chapter 12, pp 473−513.

(6) Arbogast, J. W.; Foote, C. S. *J. Am. Chem. Soc.* **1991**, *113*, 8886.

(7) Sension, R. J.; Szarka, A. Z.; Smith, G. R.; Hochstrasser, R. M. *Chem. Phys. Lett.* **1991**, *185*, 179.

(8) Ghosh, H. N.; Pal, H.; Sapre, A. V.; Mittal, J. P. *J. Am. Chem. Soc.* **1993**, *115*, 11722.

(9) Steren, C. A.; von Willigen, H.; Biczók, L.; Gupta, N.; Linschitz, H. *J. Phys. Chem.* **1996**, *100*, 8920.

(10) Fukuzumi, S.; Suenobu, T.; Patz, M.; Hirasaka, T.; Itoh, S.; Fujitsuka, M.; Ito, O. *J. Am. Chem. Soc.* **1998**, *120*, 8060.

(11) Ito, O.; Sasaki, Y.; El-Khouly, M. E.; Araki, Y.; Fujitsuka, M.; Hirao, A.; Nishizawa, H. *Bull. Chem. Soc. Jpn.* **2002**, *75*, 1247.

(12) Onodera, H.; Araki, Y.; Fujitsuka, M.; Onodera, S.; Ito, O.; Bai, F.; Zheng, M.; Yang, J.-L. *J. Phys. Chem. A* **2001**, *105*, 7341.

(13) Sandanayaka, A. S. D.; Araki, Y.; Luo, C.; Fujitsulka, M.; Ito, O. *Bull. Chem. Soc. Jpn.* **2004**, *77*, 1313.

(14) Sandanayaka, A. S. D.; Watanabe, N.; Ikeshita, K.-I.; Araki, Y.; Kihara, N.; Furusho, Y.; Ito, O.; Takata, T. *J. Phys. Chem. B* **2004**, *109*, 2516.

(15) Sandanayaka, A. S. D.; Sasabe, H.; Araki, Y.; Furusho, Y.; Ito, O.; Takata, T. *J. Phys. Chem. A* **2004**, *108*, 5145.

(16) Yahata, Y.; Sasaki, Y.; Fujitsuka, M.; Ito, O. *J. Photosci.* **2000**, *6*, 117.

(17) Okamoto, T.; Kozaki, M.; Doe, M.; Uchida, M.; Wang, G.; Okada, K. *Chem. Mater.* **2005**, *17*, 5504.

(18) Jenekhe, S. A.; Lu, L. D.; Alam, M. M. *Macromolecules* **2001**, *34*, 7315.

(19) Fungo, F.; Jenekhe, S. A.; Bard, A. J. *Chem. Mater.* **2003**, *15*, 1264.

(20) Sun, X.; Liu, Y.; Xu, X.; Yang, C.; Yu, G.; Chen, S.; Zhao, Z.; Qiu, W.; Li, Y.; Zhu, D. *J. Phys. Chem. B* **2005**, *109*, 10786.

(21) Sasaki, Y.; Araki, Y.; Ito, O.; Alam, M. M. *Photochem. Photobiol. Sci.* **2007**, *6*, 560.

(22) Islam, D.-M. S.; Sasaki, Y.; Kawauchi, H.; Kozaki, M.; Araki, Y.; Ito, O.; Okada, K. *Bull. Chem. Soc. Jpn.* **2008**, *81*, 103.

(23) (a) Yonemura, H.; Tokudome, H. N.; Yamada, S. C. *Chem. Phys. Lett.* **2001**, *346*, 361–367. (b) Yoneyama, H.; Noda, M.; Hayashi, K.; Tokudome, H.; Moribe, S.; Yamada, S. *Mol. Phys.* **2002**, *100*, 1395–1403.

(24) Okamoto, T.; Kuratsu, M.; Kozaki, M.; Hirotsu, K.; Ichimura, A.; Matsushita, T.; Okada, K. *Org. Lett.* **2004**, *6*, 3493.

(25) Maggini, M.; Scorrano, G.; Prato, M. *J. Am. Chem. Soc.* **1993**, *115*, 9798.

(26) Mečiarová, M.; Toma, Š.; Magdolen, P. *Synth. Commun.* **2003**, *33*, 3049.

(27) (a) Rehm, D.; Weller, A. *Isr. J. Chem.* **1970**, *8*, 259. (b) Lor, M.; Viaene, L.; Pilot, R.; Fron, E.; Jordens, S.; Schweitzer, G.; Weil, T.; Müllen, K.; Verhoeven, J. W.; Van der Auweraer, M.; De Schryver, F. C. *J. Phys. Chem. B* **2004**, *108*, 10721.

(28) Sasaki, M.; Shibano, Y.; Tsuji, H.; Araki, Y.; Tamao, K.; Ito, O. *J. Phys. Chem. A* **2007**, *111*, 2973.

(29) Nakamura, T.; Fujitsuka, M.; Araki, Y.; Ito, O.; Ikemoto, J.; Takimiya, K.; Aso, Y.; Otsubo, T. *J. Phys. Chem. B* **2004**, *108*, 10700.

(30) Luo, C.; Guldi, D. M.; Imahori, H.; Tamaki, K.; Sakata, Y. *J. Am. Chem. Soc.* **2000**, *122*, 6535.

(31) (a) Okada, T.; Karaki, I.; Matsuzawa, E.; Mataga, N.; Sakata, Y.; Misumi, S. *J. Phys. Chem.* **1981**, *85*, 3957. (b) van Willigen, H.; Jones, G., II; Farahat, M. S. *J. Phys. Chem.* **1996**, *100*, 3312. (c) Gould, I. R.; Boiani, J. A.; Gaillard, E. B.; Goodman, J. L.; Farid, S. *J. Phys. Chem. A* **2003**, *107*, 3515.

(32) (a) Birks, J. B. In *Photophysics of Aromatic Molecules*; Wiley: London, 1970; Chapter 7. (b) Yatsuhashi, T.; Inoue, H. *J. Phys. Chem. A* **1997**, *101*, 8166.

(33) Asahi, T.; Ohkohchi, M.; Matsusaka, R.; Mataga, N.; Zhang, R. P.; Osuka, A.; Maruyama, K. *J. Am. Chem. Soc.* **1993**, *115*, 5665.

(34) Luo, C.; Fujitsuka, M.; Huang, C.-H.; Ito, O. *J. Phys. Chem. A* **1998**, *102*, 8716.

(35) Marcus, R. A.; Sutin, N. *Biochim. Biophys. Acta* **1985**, *811*, 265.

(36) Imahori, H.; Hagiwara, K.; Akiyama, T.; Akoi, M.; Taniguchi, S.; Okada, S.; Shirakawa, M.; Sakata, Y. *Chem. Phys. Lett.* **1996**, *263*, 545.

(37) Verhoeven, J. W. *J. Photochem. Photobiol., C* **2006**, *7*, 40.

(38) Wasielewski, M. R. *J. Org. Chem.* **2006**, *71*, 5051.

JP800716E